Testing Leptonic Models for AGN Jets with the GLAST LAT

Jennifer Carson and Jim Chiang, Stanford Linear Accelerator Center, USA

We present simulated GLAST LAT spectra and analyses for three AGN for which detailed leptonic modeling exists: the flat spectrum radio quasar (FSRQ) 3C 279, the low-frequency-peaked BL Lac object (LBL) W Comae, and the high-frequency-peaked BL Lac object (HBL) Markarian 501. For each source, we consider time-averaged spectra based on detailed leptonic models that include both synchrotron self-Compton (SSC) and external Compton (EC) emission. We show the sensitivity of the LAT for >1 week of observations, assuming that GLAST is operating in its normal survey mode. These results do not assume any pointed observations or require any special scheduling.

The Models

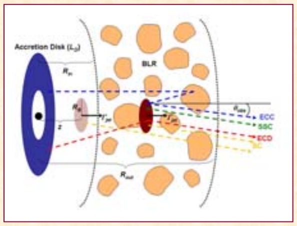

The model of Böttcher *et al.* (1997) and Böettcher & Bloom (2000) form the basis for these analyses. In this model, pair plasma blobs of radius R_B are instantaneously injected at a height z above the accretion disk (luminosity L_D) into an existing cylindrical jet structure with bulk Lorentz factor Γ_{jet} and magnetic field B. The electrons are injected with a power-law distribution $dn/d\gamma = n_e \gamma^{-p}$ with comoving density n_e, index p, and low- and high-energy bounds γ_1 and γ_2, respectively. The following radiation processes are included (see left figure): synchrotron emission (SC), inverse-Compton scattering of synchrotron photons (SSC), inverse-Compton scattering of radiation from the accretion disk entering the jet directly (ECD), and inverse-Compton scattering of accretion disk radiation scattered off broad-line region clouds (ECC). Each of these cooling mechanisms is followed self-consistently.

	L_D (erg s^{-1})	θ (deg)	τ_{BLR}	R_{in} (pc)	R_{out} (pc)	z (pc)	R_B (cm)	B (G)	γ_1	Γ_{jet}
3C 279	10^{46}	2	0.003	0.1	0.4	0.025	6×10^{16}	1.5	free	free
W Comae	10^{45}	1	free	0.2	0.25	?	10^{16}	free	free	free
Mrk 501	N/A	2	N/A	N/A	N/A	?	3×10^{15}	0.05	300	25

The table above lists the parameter values that are fixed for each model. n_e, p, and γ_2 were free parameters in every model; typical values of these parameters are $n_e \sim$ 10-50 cm^{-3}, $p \sim$ 2-3, and $\gamma_2 \sim 10^7$.

Model Spectra

We simulated a month of LAT observations for 3C 279 and W Comae and a week for Markarian 501, assuming the telescope is operating in its normal survey mode. The input models were taken from the literature, and the simulation exposure times were chosen to match the input models and the data on which they relied. The published spectra (models and data) and their references are shown below. Galactic and extragalactic diffuse emissions were also included in the simulations.

Simulated X-ray and Gamma-ray Counts

Below we present the binned counts for the simulated LAT observations, along with simulated BeppoSAX counts. The latter represent seven hours of hard x-ray data simulated using the Xspec and the BeppoSAX PDS response matrices and background model files available from the BeppoSAX public ftp site, ftp://ftp.asdc.asi.it/pub/sax/. The LAT data points were obtained by extracting events within a 3 degree radius acceptance cone centered on the target source position. A background counts model was obtained similarly by extracting from the LAT diffuse emission alone.

Likelihood Analysis

Maximum likelihood fitting is the foundation of LAT data analyses (e.g., detecting sources, determining source intensities, fitting spectral parameters, setting upper limits). The likelihood is the probability of the data (the counts that were detected) given the model (the photon sources). Evaluating the likelihood then proceeds by breaking the space into bins, and calculating the probability of the detected counts in each bin. Source confusion requires that the calculation consider several sources simultaneously, including both point sources and diffuse emission. "1-sigma" errors on fit parameters are determined by considering a change in the log-likelihood of ½ from the value the function attains at its maximum and by determining the corresponding change required in the parameter value of interest.

3C 279

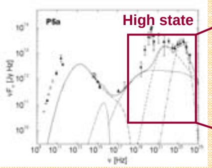

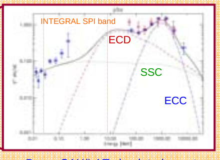

x BeppoSAX/LAT simulated counts
◇ EGRET data

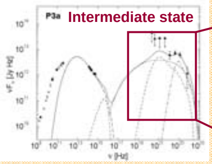

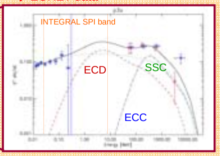

When the source is in a high state (top left), the LAT counts trace the structure in the high-energy peak. The EGRET data lacked the precision necessary to do this.

When the source is in an intermediate state (bottom left), the LAT measurement is more precise than the EGRET one, but not sufficient to model a more complicated spectrum than a simple log-parabola.

In both states, hard X-ray data (from BeppoSAX or ASTROSAT) can constrain the SSC component independently of the LAT data. Soft gamma-ray coverage, as might be provided by, e.g., INTEGRAL SPI, could independently constrain the ECD peak.

We fit the high-state data to a model with three free parameters: the normalizations of the three radiation components. The figure below shows the fit results with 1σ error bars.

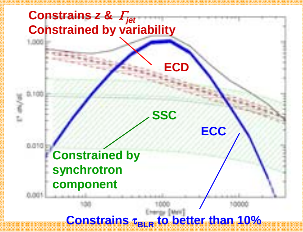

With likelihood analysis, we can easily distinguish the separate contributions from different radiation processes.

The ECD component (red band) depends primarily on z and Γ_{jet}; **LAT measurements of the ECD emission better constrain z and Γ_{jet}.** Short-term variability measurements can independently constrain these parameters.

For a given L_D, $dn/d\gamma$, and Γ_{jet}, the intensity of the ECC component (blue band) is dominated by one parameter, τ_{BLR}. Assuming the other parameters are constrained by simultaneous observations in other wavebands, **the likelihood analysis constrains the ECC normalization, and hence τ_{BLR}, to ~6%.**

The SSC component (green band) can be independently constrained by x-ray measurements.

W Comae

No EC radiation

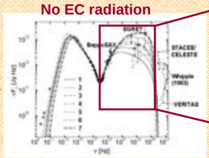

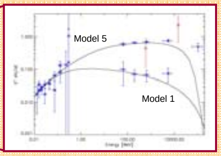

x BeppoSAX/LAT simulated counts
◇ EGRET data

Including EC radiation

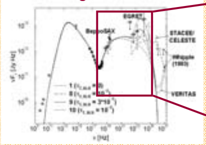

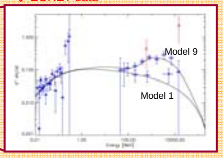

We simulated three of the 10 models shown to the far left, two without a component from external Compton emission (Models 1 and 5, top left), and one with a Thompson depth of the broad line region $\tau_{BLR}=3\times10^{-3}$ (Model 9, bottom left). Models 5 and 9 were considered the best fits to the EGRET data (red diamonds), and Model 1 represents a low flux state.

The LAT detection is much more precise than the EGRET one, even in a low state with no external Compton contribution (Model 1).

X-ray observations alone allow for a wide variety of possible model parameters. LAT observations are necessary to break the model degeneracies.

These data were fit to the cumulative model; the one free parameter is the overall normalization. The figure below shows the fit results and 3σ errors for each of the models considered.

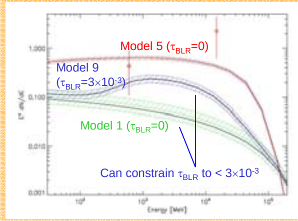

Models 1 (green) and 9 (blue) differ only in the strength of the ECC component; τ_{BLR}=0 for M1 and $\tau_{BLR}=3\times10^{-3}$ for M9. **Likelihood can easily distinguish between these two models, constraining τ_{BLR} to <3×10^{-3}.**

For the Γ_{jet} adopted by Böttcher *et al.*, Models 1 (green) and 5 (red) correspond to the smallest and largest values that γ_1 can have and still fit the optical through X-ray data, allowing the other parameters, n_e, p, γ_2, and B, to vary. For the range of indices that they find, p = 2.2 - 2.7, γ_1 is roughly the characteristic energy of the injected electrons. **Constraining γ_1 with LAT observations thus constrains the acceleration processes for these particles.**

Markarian 501

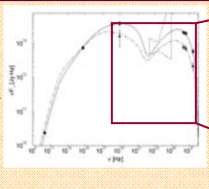

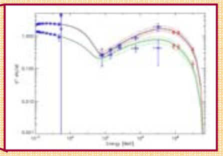

To the left, the 3σ likelihood bands for the low (green) and high (red) states are shown along with the binned counts.

x BeppoSAX/LAT simulated counts
◇ HEGRA data

In the absence of simultaneous coverage below 800 GeV, the model fits to the X-ray and TeV data (black lines) cannot constrain γ_1 and B, and so these parameters were fixed at nominal values. **Having LAT coverage down to 30 MeV frees those parameters and allows for a much more complete exploration of the parameter space. Also, measuring the full shape of the high-energy peak reveals the overall energy budget and the relative contributions of the SSC and SC cooling mechanisms. This ratio further constrains the model parameters.**